Int. J. Hyperthermia, December 2008; 24(8): 663–674

informa
healthcare

Relation between body size and temperatures during locoregional hyperthermia of oesophageal cancer patients

P. M. A. VAN HAAREN[1], M. C. C. M. HULSHOF[1], H. P. KOK[1], S. OLDENBORG[1], E. D. GEIJSEN[1], J. J. B. VAN LANSCHOT[2,3], & J. CREZEE[1]

Departments of Radiation Oncology[1] and surgery[2], Academic Medical Centre, University of Amsterdam, The Netherlands, and [3]Erasmus Medical Centre, Rotterdam, The Netherlands

(Received 11 January 2008; accepted 16 May 2008)

Abstract

Purpose. To analyse the relation between patients' body size and temperatures during locoregional hyperthermia for oesophageal cancer.

Methods. Patients were treated with neo-adjuvant chemoradiotherapy plus hyperthermia, given with the AMC-4 waveguide system. Temperatures were measured at tumour location in the oesophageal lumen using multisensor thermocouple probes. Systemic temperature rise (ΔT_{syst}) was monitored rectally. Steady-state tumour temperatures were expressed in terms of T_{90}, T_{50} and T_{10}, averaged over the five hyperthermia sessions, and correlated with patients' body mass, dorsoventral and lateral diameter and fat layer thickness, measured at tumour level using a CT scan made in treatment position. Fat percentage (*Fat*%) was estimated using diameters and fat layer thickness. Effective tumour perfusion (W_b) was estimated from the temperature decay during the cool-down period.

Results. Temperatures were inversely related to body mass, diameters, fat layer thickness, and fat percentage. The strongest univariate correlations were found with lateral fat layer thickness, lateral diameter, and body mass. An increase in lateral diameter (28→42 cm), or in lateral fat layer thickness (0→40 mm) or in body mass (50→120 kg) all yielded a ~1.5°C decrease in tumour temperature rise. Multivariate correlation analysis proved that the combination of *Fat*%, ΔT_{syst} and W_b was most predictive for the achieved tumour temperatures, accounting for 81 ± 12% of the variance in temperatures.

Conclusions. Intra-oesophageal temperatures during locoregional hyperthermia are inversely related to patients' body size parameters, of which fat percentage is the most significant prognostic factor. These findings could be used to define inclusion criteria of new studies on intrathoracic hyperthermia.

Keywords: *Intra-oesophageal temperatures, oesophageal cancer, locoregional hyperthermia, body mass, fat percentage*

Introduction

Hyperthermia is the application of elevated temperatures to tumours and is applied to improve the effectiveness of radiotherapy and/or chemotherapy. Several thermal dose expressions have been formulated over the years, reflecting different aspects of the anti-tumour mechanisms induced by hyperthermia treatment, ranging from microscopic to macroscopic effects. Hyperthermia treatment traditionally aimed at achieving tumour temperatures in the order of 43°C for 1 h, which is associated with processes like DNA damage and impaired DNA repair [1]. Contemporary guidelines prefer to quantify hyperthermia treatment in terms of 'thermal dose', cumulative equivalent minutes (CEM) at certain tumour temperature levels, and are associated with physiological processes like radiosensitization, chemosensitization, reperfusion and reoxygenation [2–8]. A strong correlation between thermal dose and clinical outcome has been shown from clinical data [3, 5–7, 9–17], even in a prospective setting [2, 4, 8, 18, 19]. To achieve a sufficiently high and

Correspondence: P. M. A. van Haaren, PhD, Department of Radiation Oncology, Academic Medical Centre, University of Amsterdam, Meibergdreef 9, 1105 AZ Amsterdam, The Netherlands. Tel: +31-20-5666826. Fax: +31-20-6091278. E-mail: p.m.haaren@amc.uva.nl

ISSN 0265–6736 print/ISSN 1464–5157 online
DOI: 10.1080/02656730802210448

uniform temperature rise in the tumour is therefore important, and remains a challenge during clinical hyperthermia [10, 20–24], especially for deep-seated tumours such as in the oesophagus.

In the Academic Medical Centre (AMC) Amsterdam, a feasibility study has been performed applying neo-adjuvant locoregional hyperthermia in combination with concurrent chemotherapy in patients with operable oesophageal cancer [25]. Hyperthermia proved to be feasible for treatment of these patients and the clinical results were promising. Consequently, a phase II study for patients with oesophageal cancer was conducted in the AMC, applying neo-adjuvant radiotherapy combined with weekly locoregional hyperthermia with concurrent chemotherapy. In both studies, hyperthermia was administered using the AMC-4 waveguide system [26]. The achieved temperatures were generally lower than originally aimed for: in the feasibility study an average median tumour temperature (T_{50}) of 40°C was achieved and a minimal tumour temperature (T_{90}) of only 39.3°C [25]. Nevertheless, clinical outcome was unexpectedly good, with a 2-year survival rate of 62% [25]. These findings are further supported by good preliminary results of the current phase II study, with a 91% survival rate at a median follow-up of 9 months [27].

The achieved tumour temperature distribution depends on many different factors, some of which are difficult to modify or manipulate. The power distribution in the patient and the amount of power deposited in the target region are dependent on the power steering capabilities of the hyperthermia device and the ability to avoid or reduce the influence of treatment-limiting hotspots in normal tissue. In turn, the patient-specific anatomy is of great influence on the local power distribution [28], whereas the thermal properties of different tissues, especially perfusion, have a major impact on the resulting temperature distribution [29]. Furthermore, one can imagine that other patient-specific characteristics, such as body diameters, body mass, the amount of subcutaneous fat tissue, and the general capability of the patient to remove heat from the body by thermal conduction, transpiration and heat radiation, can also have a significant influence on the achieved temperature distribution in the patient.

In this study, relations between parameters characterizing the patients' body size (mass, diameters, fat percentage) and hyperthermia treatment quantities (temperatures, perfusion), were examined for the patients treated in the phase II study. It was hypothesized that beyond certain dimensions of the patient's body, it may be difficult to accomplish effective tumour temperatures. These findings could be of influence on inclusion criteria for new studies on intrathoracic hyperthermia.

Patients and methods

Patients

A phase II study for the treatment of stage II or III operable oesophageal adenocarcinoma or squamous cell carcinoma was started at the AMC in August 2003. In this study, neo-adjuvant radiotherapy was applied in combination with weekly locoregional hyperthermia and concurrent chemotherapy. Radiotherapy (41.4 Gy) was given in 23 daily fractions of 1.8 Gy, starting on a Monday or Tuesday. Hyperthermia was given once weekly, for 5 weeks, on Monday or Tuesday. Chemotherapy (carboplatin and paclitaxel) was given once weekly, on the same day as the hyperthermia treatment. On such a 'triple' treatment day, first paclitaxel (50 mg/m^2) was administered to the patient, followed by radiation treatment. Next, the patient was transported to the endoscopy department, for placement of a balloon catheter at the tumour level under endoscopic guidance (see Hyperthermia treatment and measurements). The patient was transported back to the radiotherapy department for hyperthermia treatment, which started typically one hour after radiotherapy. Carboplatin (AUC = 2) was administered simultaneously with the hyperthermia treatment. An oesophageal resection was performed 4–6 weeks after completion of the neo-adjuvant treatment. Tumour pathology status was determined from the resection and classified according to complete remission (CR), partial remission with only residual microscopic tumour foci (mPR), partial remission (PR), or stable disease (StD). Until now, 29 patients have been treated, with a median tumour length of 6 cm (range 2–12 cm) at the start of the first hyperthermia treatment. All tumours were located below carina level, and cardia extension was limited to 2 cm. Pre-treatment tumour stage consisted mainly of T3 tumours (86%) and N+ disease (66%).

Hyperthermia treatment and measurements

Hyperthermia treatments were performed using the 70MHz AMC-4 phased array system [30]. Patients were treated in prone position. Temperatures were monitored rectally, intra-oesophageally and intramuscularly near the spine, using multisensor copper-constantan thermocouple (TC) probes. Systemic temperature was monitored rectally with a 14-point TC (spacing 1 cm) inside a closed-end thermometry catheter. Oesophageal tumour temperatures were measured using two 21-point TCs (spacing 1 cm) mounted on opposite sides of an

inflatable balloon catheter (length 6 or 8 cm, diameter 1 cm) for optimal intraluminal fixation and contact with the tumour [31]. The balloon catheter was placed at the tumour level under endoscopic guidance prior to each hyperthermia treatment session. There was also an E-field probe mounted on the balloon catheter for E-field measurements and adjustment of the antenna settings of the AMC-4 system. Clinical experience has led to standard power settings of the four antennas of the AMC-4 system for specific tumour sites. For treatment of oesophageal tumours a power ratio between top, bottom, left and right antenna of 1:3:3:3 is used. The top antenna, which is closest to the spine, delivers less power to prevent overheating of the spinal cord. A total power of 800 W is applied to the four antennas, which results in an effective output power (P_{AMC4}) of 440 W, including the actual efficiency of the AMC-4 system [32]. Phase settings are optimized such that a maximal E-field is measured by the E-field probe at the tumour location, whereby the top antenna serves as reference (i.e. phase 0°). During the hyperthermia treatment, temperatures were measured every 30 s, during a 5-s power-off period of the AMC-4 system, to avoid electromagnetic (EM) disturbances of the thermometry [33]. According to protocol, the steady-state period of 60 min (3600 s) started when at least one of the tumour measurement points reached 41°C, or alternatively after an induction period of 30 min. At the end of the steady-state period, the power of the AMC-4 system was switched off, and the temperature measurements continued every 5s for a period of 2 min, in order to quantify the temperature decay.

For treatment planning purposes [34], a CT scan of all patients in this study was made in hyperthermia treatment position, i.e. in prone position on a water bolus and mattresses, as used during hyperthermia treatments (Figure 1, left). Using this CT scan, the patients dorsoventral or anterior-posterior (AP), and lateral (LAT) diameters were determined at mid-tumoural level. Furthermore, the thickness of all subcutaneous fat layers at the dorsal, ventral, left and right side of the patient were measured in the same CT slice. The fat layers can be easily distinguished on the CT scans based on the contrast in Hounsfield units between different tissue types [35]. The patients' body mass was determined weekly during the pre-operative treatment period. Body mass remained fairly stable for most patients; the average weight loss during 5 weeks was only 0.9 ± 2.4 kg, i.e. only $1.4 \pm 3.7\%$. Therefore, the average body mass over these 5 weeks was used in this study.

Temperature analysis in relation to body size parameters

A simplified model for heating a certain amount of tissue yields

$$m \cdot c \cdot \Delta T = E_{in} = P_{eff} \cdot \Delta t \rightarrow \Delta T = \frac{P_{eff} \cdot \Delta t}{m \cdot c} \quad (1)$$

with m the mass of the heated amount (kg), c the specific heat capacity ($\sim 3600\,J\,kg^{-1}{}^{\circ}C^{-1}$), ΔT the temperature rise (°C) with respect to the basal temperature, E_{in} the total absorbed energy (J), P_{eff} the total effective absorbed power (W), and Δt the duration of heating ($\sim$3600 s). Equation 1 predicts that the temperature rise ΔT is inversely proportional to the mass m. Applying this to the whole patient, the effective power P_{eff} can be written in terms of the power delivered to the patient by the AMC-4 hyperthermia system (P_{AMC4}, 440 W) minus the power removed from the patient due to all cooling processes together (P_{cool}), such as thermal

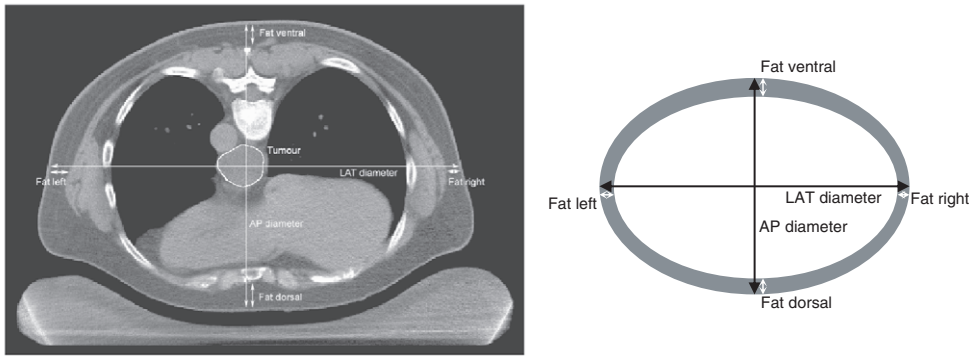

Figure 1. Left: Transversal slice of a CT scan of an oesophageal cancer patient, made in treatment position, i.e. in prone position on a water bolus. The tumour was outlined by a radiation oncologist. The dorsoventral (AP) and lateral (LAT) diameters, as well as the thickness of the dorsal, ventral, left and right fat layers were measured at mid-tumoural level. Right: Schematic drawing of the patient's cross section based on the diameters and fat layer thickness as determined from the CT scan, used to estimate the fat percentage.

conduction, bolus cooling, transpiration, and heat radiation: $P_{\text{eff}} = P_{\text{AMC4}} - P_{\text{cool}}$. Within this concept, one can define a so-called 'cooling capacity' (*CC*) of the patient, expressing the capability of an individual patient to remove power from the body: $CC \equiv 100\% \cdot P_{\text{cool}}/P_{\text{AMC4}}$. This implies $P_{\text{eff}} = P_{\text{AMC4}} \cdot (100\% - CC)$, and, consequently, $\Delta T = P_{\text{AMC4}} \cdot (100\% - CC)/m$. Note that perfusion basically does not contribute to this *CC*-concept, since by perfusion heat is only (re)distributed over the body as a whole, thus perfusion is not responsible for heat removal from the body.

Simplifying the patient to a homogeneous volume $V(\text{m}^3)$, the body mass can be estimated using

$$m = \rho \cdot V \approx \text{Constant} \cdot l \cdot AP \cdot LAT \qquad (2)$$

with ρ the density (kg m^{-3}), l the length (m), AP the dorsoventral diameter (m), and LAT the lateral diameter (m). Combining Equations 1 and 2 implies that the temperature rise ΔT can also be considered inversely proportional to the AP and LAT diameters. Therefore the relations between tumour temperatures (see below) and body size parameters were fitted with first order inverse functions.

Predicting the influence of the subcutaneous fat layers on temperatures in the target region is complicated. Firstly, fat has a low relative permittivity (~10 [36, 37]), which results in sub-optimal coupling of the 70 MHz radiation from the antennas of the hyperthermia system into the patient. Secondly, fat has also a low thermal conductivity (~0.22 W m^{-1}°C^{-1} [36]), thus the fat layers act as a thermal isolation for the heated region inside the patients body. Thirdly, for an increasing fat layer thickness the distance between antennas and the target region increases, which may result in a sub-optimal cooperation of the four antennas.

Estimation of fat percentage

The patients' fat percentages were estimated using a simplified representation of the patients' cross section from the same CT slice, from which the AP and LAT diameters and the thickness of the subcutaneous fat layers had been determined. The (cross-sectional) fat percentage (*Fat*%) was estimated using the surface areas (*A*) of the two ellipses as shown in Figure 1 (right):

$$\begin{aligned} Fat\% &= 100\% \cdot \frac{A_{\text{fat}}}{A_{\text{patient}}} \\ &= 100\% \cdot \frac{\left\{ \begin{array}{c} AP \cdot LAT - (AP - fat_{\text{AP}}) \\ \cdot (LAT - fat_{\text{LAT}}) \end{array} \right\}}{AP \cdot LAT} \end{aligned} \qquad (3)$$

with $A_{\text{fat}}/A_{\text{patient}}$ the area fraction of fat tissue in the simplified cross-section of the patient, fat_{AP} the total thickness of all dorsoventral fat layers and fat_{LAT} the total thickness of all lateral fat layers.

Estimation of effective tumour perfusion

The local temperature (T(°C)) development during hyperthermia treatments can be described by Pennes' bioheat transfer equation [38]. For homogeneous tissue this energy balance is

$$\rho_t c_t \frac{\partial T}{\partial t} = \nabla \cdot (k_t \nabla T) - c_b W_b (T - T_{\text{art}}) + P \qquad (4)$$

with ρ_t the tissue density (kg m^{-3}) and c_t the specific heat capacity (J kg^{-1}°C^{-1}). The first term on the right represents the conduction in tissue, with k_t the thermal conductivity of tissue (Wm^{-1}°C^{-1}). The second term on the right represents the perfusion, with c_b the specific heat of blood, W_b the volumetric perfusion rate of tissue (kg m^{-3} s^{-1}), and T_{art} the arterial temperature, which is usually taken equal to the body core temperature T_{basal} (37°C). The absorbed power density is represented by P(Wm^{-3}). Perfusion is expected to be the dominant mechanism for heat removal from the target region; the contribution of conduction can be incorporated into an 'effective perfusion' term [24].

In order to estimate this effective perfusion in the target region for individual patients, temperature measurements are continued during a 2-min cool-down period after switching the power off ($P = 0$) at the end of the steady-state period (Figure 2a). An exponentially decaying temperature during this cool-down period was assumed:

$$T(t) = T_{\text{basal}} + \Delta T_{\text{SST}} \cdot \exp(-t/\tau) \qquad (5)$$

with T_{basal} the basal body core temperature (37°C), ΔT_{SST} the temperature rise (°C) with respect to T_{basal} at the end of the steady-state period, *i.e.* at the beginning of the cool-down period, and τ the time constant (s) of the exponential decay (Figure 2b). Substitution of Equation 5 in Equation 4 gives for the cool-down period:

$$\begin{aligned} &\rho_t c_t \cdot \frac{-\Delta T_{\text{SST}}}{\tau} \cdot \exp(-t/\tau) \\ &\quad = -c_b W_b \cdot \Delta T_{\text{SST}} \cdot \exp(-t/\tau) \end{aligned} \qquad (6)$$

thus the relation between the effective perfusion rate W_b and the time constant τ of the temperature decay would be

$$W_b = \frac{\rho_t c_t}{c_b \tau} \qquad (7)$$

For tumour tissue $\rho_t = 1050$ kg m^{-3}, $c_t = 3639$ J kg^{-1}°C^{-1}, $c_b = 3840$ J kg^{-1}°C^{-1} [36], resulting in $W_b = 995/\tau$. Perfusion calculated this way can be seen as an 'effective perfusion', responsible for heat removal from the target region, and in which the

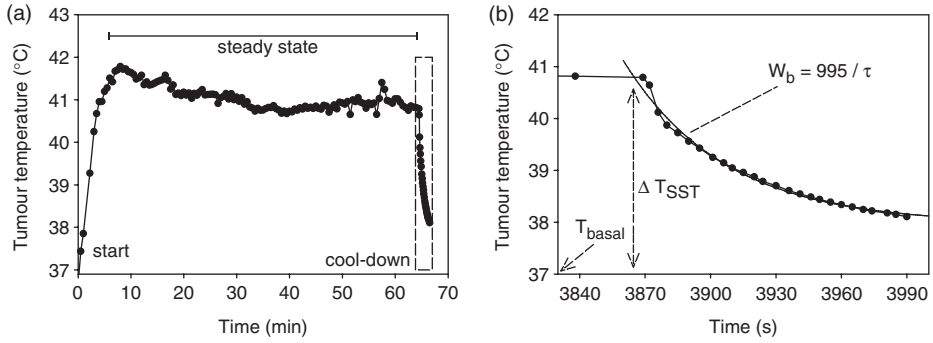

Figure 2. (a) Example of the estimation of effective perfusion from tumour temperature measurements during the 2-min cool-down period following the 60-min steady-state period. (b) The temperature decrease during the cool-down period was fitted with an exponential decay (Equation 5), from which the effective perfusion was determined according to Equation 7.

contribution of conduction and cooling by heart, lungs and large blood vessels has been accounted for.

Statistics

The correspondence between different parameters was expressed in terms of the univariate correlation coefficient *R*. Multivariate correlation analyses were performed using SPSS 12. The correlation coefficient squared (R^2) quantifies the amount of explained variance. Relations between different parameters were fitted with linear or first order inverse functions, using SigmaPlot 2000. Similar to R^2, the measure R^2_{fit} is used to quantify the quality of model fits. Tumour temperatures were quantified by T_{90}, T_{50} and T_{10}, the temperature at least achieved in 90%, 50% and 10% of the tumour, respectively. Tumour temperatures for the different tumour pathology groups were compared using ANOVA with a Bonferroni post-hoc test. A value of $p < 0.05$ was considered significant. Data are presented as mean ± *SD*, unless otherwise stated.

Results

Patients' characteristics

Mean body size characteristics, hyperthermia treatment results and estimated effective tumour perfusion for all 29 patients are summarized in Table I. Of all 29 patients, 27 underwent surgical resection of the oesophagus. In one patient progressive disease was diagnosed, and one patient died of pulmonary embolism, both prior to surgery after completion of the neo-adjuvant treatment. For the 27 pathologically evaluable patients, response rates were CR: 5 pts (19%), mPR: 7 pts (26%), PR: 9 pts (33%) and StD: 6 pts (22%). The average tumour temperatures achieved during the hyperthermia treatments classified by the different pathological responses are shown in Figure 3. Although there were no significant differences in temperatures between the different groups of patients, these data do suggest a dose-effect relation of the hyperthermia treatment.

Table I. Patients characteristics and hyperthermia treatment results for all 29 patients.

Patient and treatment characteristics	Mean ± *SD*
Dorsoventral diameter, AP (cm)	25.2 ± 2.7
Lateral diameter, LAT (cm)	34.7 ± 3.3
Body mass, M (kg)	81.6 ± 18.0
Dorsal fat layer(s) (mm)	7.3 ± 4.2
Ventral fat layer(s) (mm)	12.7 ± 7.7
Total dorsoventral fat layers, fat_{AP} (mm)	20.0 ± 11.2
Left fat layer(s) (mm)	8.2 ± 4.2
Right fat layer(s) (mm)	8.3 ± 6.1
Total lateral fat layers, fat_{LAT} (mm)	16.6 ± 9.7
Fat percentage, *Fat*% (%)	11.9 ± 5.9
Minimal temperature, T_{90} (°C)	38.6 ± 0.5
Median temperature, T_{50} (°C)	39.2 ± 0.6
Maximal temperature, T_{10} (°C)	40.1 ± 0.8
Systemic temperature rise, ΔT_{syst} (°C)	1.1 ± 0.4
'Effective'perfusion, W_b (kg m^{-3} s^{-1})	13.5 ± 3.6

Relation between fat layers, fat percentage, body diameters and body mass

The thickness of the total dorsoventral (AP) fat layers (dorsal plus ventral) was proportionally related to the dorsoventral diameter, and the thickness of the total lateral (LAT) fat layers (left plus right) was proportionally related to the lateral diameter. The thickness of both total dorsoventral and total lateral fat layers, as well as the estimated fat percentage, were proportionally related to body mass.

Relation between tumour temperatures, diameters, body mass, fat layers and fat percentage

All tumour temperatures, quantified by T_{90}, T_{50}, and T_{10} were inversely related to dorsoventral (AP) and

lateral (LAT) diameters as well as to body mass. The relations between T_{50} and AP diameter, LAT diameter and body mass, fitted with first order inverse functions, are shown in Figure 4. The dependence of T_{50} on the body size parameters was substantial: an increase in dorsoventral diameter from 20 to 32 cm (i.e. 60% increase) yielded a decrease in temperature rise of ~1°C (i.e. ~50% decrease with respect to the basal body temperature of 37°C); an increase in lateral diameter from 28 to 42 cm (50% increase) yielded a decrease in temperature rise of ~1.5°C (~60% decrease); and an increase in body mass from 50 to 120 kg (140% increase) yielded a decrease in temperature rise of ~1.5°C (~60% decrease). These characteristics were similar for T_{90} and T_{10}.

The tumour temperatures, T_{90}, T_{50} and T_{10}, were also inversely related to the thickness of the total AP and LAT fat layers as well as to the estimated fat percentage. The relations between T_{50} and AP fat layers, LAT fat layers and fat percentage, fitted with first order inverse functions, are shown in Figure 5. Again, the dependence was substantial: an increase in dorsoventral fat layer thickness from 0 to 40 mm yielded a decrease in temperature rise of ~1.5°C (~60% decrease); an increase in lateral fat layer thickness from 0 to 40 mm yielded a decrease in temperature rise of ~1.5°C (~60% decrease); and an increase in estimated fat percentage from 0 to 25% yielded a decrease in temperature rise of ~1.5°C (~60% decrease). These characteristics were similar for T_{90} and T_{10}.

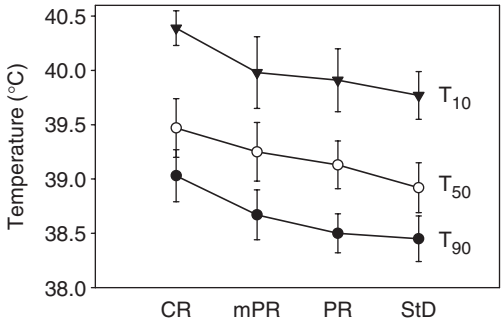

Figure 3. Average tumour temperatures, quantified by T_{90}, T_{50} and T_{10}, classified by the different pathological responses. CR, complete remission ($n=5$); mPR, partial remission with only residual microscopic tumour foci ($n=7$); PR, partial remission ($n=9$); StD, stable disease ($n=6$). Data are mean ± SEM.

Relation between tumour temperatures and systemic temperature rise

The rise in systemic temperature (ΔT_{syst}) during the hyperthermia treatment was expected to be more or less inversely related to the body mass (Equation 1). As described in the Methods, the effective power

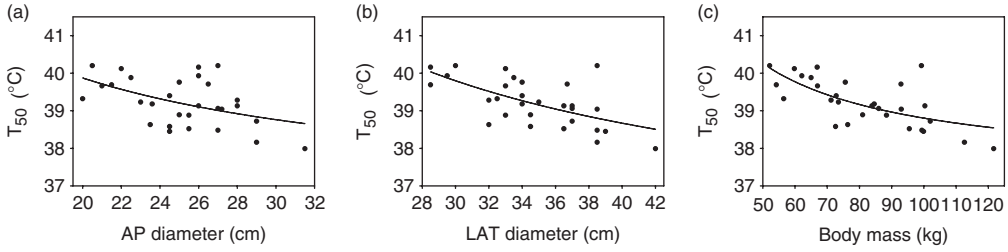

Figure 4. (a) Relation between median tumour temperature (T_{50}) and dorsoventral (AP) diameter. (b) Relation between T_{50} and lateral (LAT) diameter. (c) Relation between T_{50} and body mass. All relations were fitted with first order inverse functions (lines). R^2_{fit} was 0.23 (a), 0.38 (b) and 0.45 (c).

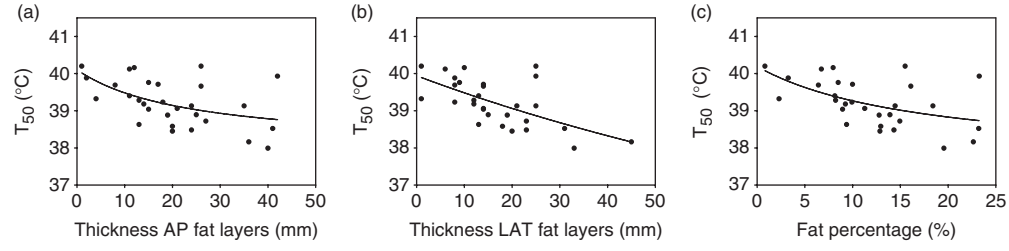

Figure 5. (a) Relation between median tumour temperature (T_{50}) and thickness of dorsoventral (AP) fat layers. (b) Relation between T_{50} and thickness of lateral (LAT) fat layers. (c) Relation between T_{50} and estimated fat percentage. All relations were fitted with first order inverse functions (lines). R^2_{fit} was 0.27 (a), 0.38 (b) and 0.27 (c).

absorbed in the patient's body depends on the power delivered to the body by the AMC-4 hyperthermia system and the power removed from the body due to cooling. Patients differ in their capability to remove heat from their body, the so-called 'cooling capacity' (*CC*). The univariate correlation between ΔT_{syst} and body mass was weak: $R = -0.42$ (Table II). This implies that there will be no clear linear relation between ΔT_{syst} and body mass for the whole group of patients. Roughly, a more or less inverse relation between ΔT_{syst} and body mass was observed for the whole group (Figure 6a), but there was a rather large spread between individual patients, indicating a relatively large variation in *CC* between the different patients. The depicted curves in Figure 6a represent the inverse relations $\Delta T_{syst} = 110$/m, and $\Delta T_{syst} = 55$/m, corresponding to cooling capacities of respectively 75%, and 87.5% (see Methods). Averaged over all 29 patients, *CC* was $81 \pm 7\%$ (range 63–92%). As mentioned in the Methods, perfusion basically does not contribute to *CC*, and is therefore expected to have hardly any influence on the systemic temperature (rise) during the hyperthermia treatment. As shown in Table II there was indeed a very weak correlation between effective perfusion and ΔT_{syst}: $R = -0.09$. In contrast, there was a rather strong, more or less proportional relation between the rise in systemic temperature (ΔT_{syst}) and the tumour temperatures T_{90}, T_{50}, and T_{10}. The relation between T_{50} and ΔT_{syst} is shown in Figure 6b, and was fitted with a linear function.

Relation between tumour and systemic temperatures and perfusion

All tumour temperatures, quantified by T_{90}, T_{50}, and T_{10} were inversely related to the effective perfusion, determined from the temperature decay during the cool-down period at the end of the hyperthermia treatment. Roughly, the systemic temperature rise (ΔT_{syst}) was also inversely related to the effective perfusion, although this relation was much weaker than for the tumour temperatures. This was already indicated by the very weak correlation between ΔT_{syst} and perfusion as mentioned above ($R = -0.09$). The relations between T_{50} and perfusion, and between ΔT_{syst} and perfusion are shown in Figure 7. The dependence of T_{50} was quite substantial: a 'doubling' in effective perfusion from 10 to 22 $\mathrm{kg\,m^{-3}\,s^{-1}}$ (120% increase) yielded

Table II. Univariate correlations between parameters for all 29 patients ($\star p < 0.05$, $\star\star p < 0.01$).

R	AP	LAT	*M*	fat_{AP}	fat_{LAT}	*Fat%*	T_{90}	T_{50}	T_{10}	ΔT_{syst}	W_b
AP	1	0.64**	0.82**	0.66**	–	0.62**	−0.49**	−0.49**	−0.51**	−0.26	–
LAT		1	0.89**	–	0.62**	0.47**	−0.66**	−0.63**	−0.57**	−0.41*	–
M			1	0.66**	0.81**	0.65**	−0.69**	−0.69**	−0.63**	−0.42*	0.30
fat_{AP}				1	0.87**	0.98**	−0.45*	−0.49**	−0.50**	−0.13	–
fat_{LAT}					1	0.91**	−0.57**	−0.62**	−0.57**	−0.32	–
Fat%						1	−0.46*	−0.50**	−0.50**	−0.13	–
T_{90}							1	–	–	0.63**	−0.36
T_{50}								1	–	0.67**	−0.26
T_{10}									1	0.59**	−0.22
ΔT_{syst}										1	−0.09
W_b											1

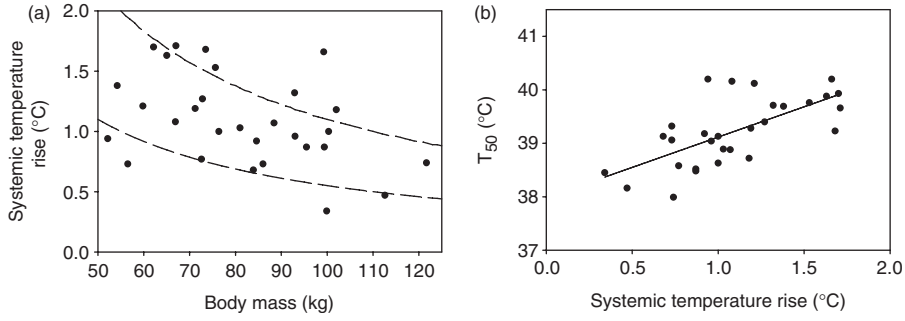

Figure 6. (a) Relation between systemic temperature rise and body mass. The depicted curves (dashed lines) represent the inverse relations $\Delta T_{syst} = 110$/m and $\Delta T_{syst} = 55$/m (see text). (b) Relation between median tumour temperature (T_{50}) and systemic temperature rise. Relation was fitted with a linear function (solid line). R^2_{fit} was 0.45.

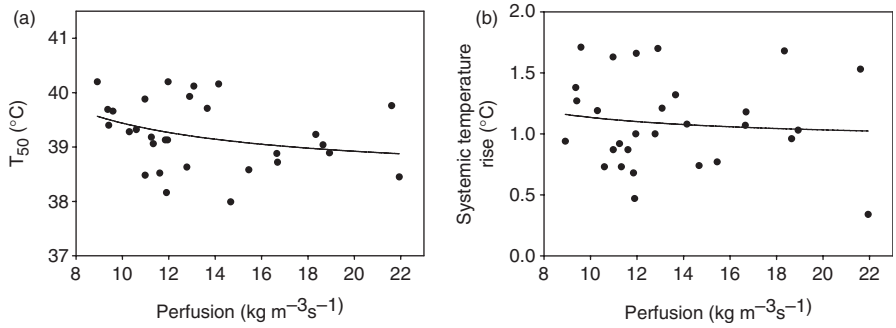

Figure 7. (a) Relation between median tumour temperature (T_{50}) and effective perfusion, as determined from the temperature decay at the end of the hyperthermia treatment. (b) Relation between systemic temperature rise and effective perfusion. Both relations were fitted with first order inverse functions (lines). R^2_{fit} was 0.10 (a) and 0.01 (b).

Table III. Multivariate correlation analysis for the three parameters that most strongly determined tumour temperatures, for all 29 patients ($\star p < 0.05$, $\star\star p < 0.01$). For comparison the univariate correlations for the concerned parameters have been reprinted from Table II. The sum of the partial correlations squared (ΣR^2) quantifies the amount of the variance in the temperatures that is explained by the three parameters. For comparison a pseudo-ΣR^2 is given for the univariate correlations.

	Univariate correlations				Multivariate correlations			
	T_{90}	T_{50}	T_{10}	Mean $\pm$ *SD*	T_{90}	T_{50}	T_{10}	Mean $\pm$ *SD*
Fat%	−0.46$\star$	−0.50$\star\star$	−0.50$\star\star$	−0.49 ± 0.02	−0.50$\star\star$	−0.56$\star\star$	−0.52$\star\star$	−0.53 ± 0.03
ΔT_{syst}	0.63$\star\star$	0.67$\star\star$	0.59$\star\star$	0.63 ± 0.04	0.66$\star\star$	0.71$\star\star$	0.61$\star\star$	0.66 ± 0.05
W_b	−0.36	−0.26	−0.22	−0.28 ± 0.07	−0.40$\star$	−0.27	−0.19	−0.28 ± 0.11
ΣR^2	(*0.73*)	(*0.77*)	(*0.64*)	(*0.71 ± 0.07*)	0.85	0.89	0.68	0.81 ± 0.12

a 'halving' in temperature rise of ~1°C (~45% decrease). These characteristics were similar for T_{90} and T_{10}.

Univariate correlations

All relevant univariate correlations (R) between the different parameters for all 29 patients are summarized in Table II. It should be noted that in the calculation of such correlations, standardly linear relations between both parameters are assumed. For some of the above mentioned relations this is a correct model (e.g. Figure 6b), but for most of the above mentioned relations this is not an optimal model (e.g. Figure 4, 5, 6a and 7). Nevertheless, these correlations do provide insight in the degree of correspondence between different parameters. Strong and significant ($p < 0.01$) correlations were found between the different parameters that quantify the patient's body size, such as body mass, dorso-ventral diameter and fat layer thickness, lateral diameter and fat layer thickness, and estimated fat percentage ($R \sim 0.6$–0.9). Regarding the tumour temperatures, quantified by T_{90}, T_{50}, and T_{10}, the strongest correlations were found with LAT fat layer thickness ($R = -0.59 \pm 0.03$), with LAT diameter ($R = -0.62 \pm 0.04$), and with body mass ($R = -0.67 \pm 0.03$). The quality of the first order inverse fits (expressed by R^2_{fit}) was on average ~50% higher than based on the univariate (linear) correlations squared, implying that ~50% more of the variance in the tumour temperatures can be explained by the patient's body size parameters using first order inverse models.

Multivariate correlation analysis

Since all body size parameters can be assumed to be interdependent to some extent, multivariate correlation analyses were performed to determine the parameters that most strongly determined the tumour temperatures, quantified by T_{90}, T_{50} and T_{10}. The combination of estimated fat percentage (*Fat%*), systemic temperature rise (ΔT_{syst}) and estimated effective tumour perfusion (W_b) proved to be most predictive for the achieved tumour temperatures (Table III). For comparison, the univariate correlations for the concerned parameters have been reprinted from Table II. The sum of the partial correlations squared (ΣR^2) quantifies the amount of the variance in the temperatures that is explained by the concerned parameters ($\Sigma R^2 = 1$ corresponds to 100% explained). Together, these three parameters were capable of explaining 85% of the variance in T_{90}, 89% of T_{50} and 68% of T_{10}, as shown in Table III. For comparison, a pseudo-ΣR^2

is given for the univariate correlations. In univariate correlations the contribution of possible mutual interactions between different parameters is not accounted for. Such a pseudo-ΣR^2 could therefore have reached >100%, however it was only $71 \pm 7\%$ for the aforementioned three parameters.

Discussion

The relation between body size characteristics and hyperthermia treatment results was studied for 29 patients with oesophageal cancer. All body size parameters were strongly correlated for all patients. The achieved tumour temperatures were inversely related to all body size parameters and to the estimated tumour perfusion.

Achieved temperatures and clinical response

The achieved tumour temperatures in oesophageal cancer patients were generally lower than originally aimed for, both in the previous feasibility study and in the current phase II study. The thermal dose delivered to the patient was limited by (in order of importance): (1) patient tolerance, in terms of systemic stress and general discomfort at high power; (2) the spinal cord, for which a constraint of 41°C was used to prevent neurotoxicity; (3) the maximal amount of power, delivered by the AMC-4 waveguide system.

Several clinical studies have shown a correlation between achieved tumour temperatures or thermal dose and clinical outcome [3, 9–17, 19]. In the present phase II study, a trend was observed between achieved tumour temperatures and pathological response (Figure 3). To achieve a sufficiently high and uniform temperature rise in the tumour is therefore important, and remains a challenge during clinical hyperthermia [10, 20–24]. Firstly, it remains technically difficult to heat oesophageal tumours with external heating devices only. Therefore, the effectiveness of an intraluminal heating technique (hot water balloon) for heating oesophageal tumours, and applied in combination with the external AMC-4 system, is currently under investigation in our institute [39]. Secondly, most patients possess a relatively high capability of removing heat from the body, reducing the effective inserted power in the body to only ~10–25%. Furthermore, there are large variations between different patients in their 'cooling capacity' (Figure 6a), and consequently in the capability of heating all patients to sufficiently high temperatures ('easy-to-heat' versus 'difficult-to-heat') [40, 41].

It remains difficult to estimate levels for the minimally required tumour temperatures to be achieved during clinical hyperthermia treatments. A widely accepted adequate hyperthermia dose is 1 hour at 43°C [1], which appears virtually unreachable with the current heating techniques within most clinical studies. Hypothesizing that tumour temperatures below 39°C may not be clinically relevant would suggest that patients with, for instance, a fat percentage of >16% should not be included in hyperthermia studies. It should, however, be noted that clinical outcome may still be positive even at lower tumour temperatures [42, 43].

Estimation of effective tumour perfusion

Several methods have been described to estimate perfusion from temperature measurements during the steady-state period and the cool-down period of hyperthermia treatment, such as fitting the thermal decay [44–49] or using iterative loops to obtain agreement between calculations and measurements [50, 51]. Generally, this is quantified in terms of some 'effective perfusion', since it is difficult to distinguish individual contributions of other local cooling processes, such as conduction or cooling by nearby large blood vessels or lungs. Upon refinement of the models and availability of more (temperature) data from the surroundings of the tumour, it may be possible to estimate individual contributions of conduction and perfusion more accurately [45–48]. In the present study, tumour perfusion was estimated from fitting the thermal decay during the cool-down period with an exponential decay model, and using the bioheat transfer equation. Perfusion calculated this way can be seen as an 'effective perfusion', responsible for heat removal from the target region, and in which the residual contribution of conduction and cooling by heart, lungs and large blood vessels has been accounted for. The reported values of the 'effective perfusion' ($13.5 \pm 3.6\,\mathrm{kg\,m^{-3}\,s^{-1}}$) are much higher than the values generally reported in literature for tumour ($\sim 1.8\,\mathrm{kg\,m^{-3}\,s^{-1}}$) or muscle-like tissue ($\sim 3.6\,\mathrm{kg\,m^{-3}\,s^{-1}}$). This is due to the fact the oesophagus is surrounded by the heart, lungs and large blood vessels (aorta and vena cava). These three will generally be at lower temperature than the tumour, and are subject to a very high blood flow (heart and aorta) or air flow (lungs). Therefore, conductive heat loss from the tumour to heart, lungs and large vessels can be substantial, and has to be incorporated in the 'effective perfusion'. For this study it was, however, not necessary to quantify exactly the individual contributions of all separate cooling processes, since it was only aimed to determine the influence of the patient-specific tumour-related cooling processes as a whole on the achieved tumour temperatures in the concerned patient.

Considerations for clinical practice

The combination of estimated fat percentage, systemic temperature rise and estimated effective tumour perfusion proved to be most predictive for the achieved tumour temperatures, explaining 81% of the variance in the temperatures.

Systemic temperature and its rise during hyperthermia treatment is dependent on the amount of power inserted in the patient's body by the heating device(s), and on the 'cooling capacity' of the patient as a whole, as discussed above. In contrast, the estimated tumour perfusion is a local parameter quantifying a tumour-related effect. However, to use its predictive value for tumour temperatures the effective perfusion should be known under hyperthermia conditions [52], since perfusion is strongly dependent on temperature [53]. The effect of perfusion on temperature is complicated, as shown by the data in Figure 7. Generally, a higher effective perfusion will result in lower temperatures, but other factors may also play a role. No matter how interesting, both systemic temperature rise and effective perfusion cannot be used as prognostic factors for hyperthermia treatment outcome, since both can only be determined under hyperthermia conditions.

Fat percentage can be determined prospectively and relatively easily, using electrical conduction measurements or skin-fold measurements, and can be considered a patient-specific total body parameter. In the present study fat percentage was estimated retrospectively using a CT scan at the tumour location, and can in this case be considered a more or less regional parameter of the part of the body that was subjected to the hyperthermia treatment. There are some other measurement techniques and/or calculation models for fat percentage available [54, 55], all using certain assumptions of body composition to be within specified ranges, but it remains the question whether these are applicable to (oesophageal) cancer patients or only to relatively healthy volunteers. Nevertheless, fat percentage proved the most significant prognostic factor for the achieved tumour temperatures. Consequently, in our institute, body mass, body mass index, body diameters, and most importantly fat percentage are now routinely measured for all patients receiving locoregional hyperthermia, using a Tanita TBF-521 body fat monitor/scale.

Conclusions

Clear inverse relations were found between intra-oesophageally measured temperatures during locoregional hyperthermia and patients' body size parameters, of which fat percentage proved to be the most significant prognostic factor. These findings could be of influence on inclusion criteria for new studies on hyperthermia in the thoracic region.

Acknowledgements

This study was supported by the Dutch Cancer Society grant 2002–2622.

Declaration of interest: The authors report no conflicts of interest. The authors alone are responsible for the content and writing of the paper.

References

1. Sapareto SA, Dewey WC. Thermal dose determination in cancer therapy. Int J Radiat Oncol Biol Phys 1984;10:787–800.
2. Leopold KA, Dewhirst MW, Samulski TV, Dodge RK, George SL, Blivin JL, Prosnitz LR, Oleson JR. Cumulative minutes with T90 greater than Tempindex is predictive of response of superficial malignancies to hyperthermia and radiation. Int J Radiat Oncol Biol Phys 1993;25:841–847.
3. Kapp DS, Cox RS. Thermal treatment parameters are most predictive of outcome in patients with single tumor nodules per treatment field in recurrent adenocarcinoma of the breast. Int J Radiat Oncol Biol Phys 1995;33:887–899.
4. Jones EL, Oleson JR, Prosnitz LR, Samulski TV, Vujaskovic Z, Yu D, Sanders LL, Dewhirst MW. Randomized trial of hyperthermia and radiation for superficial tumors. J Clin Oncol 2005;23:3079–3085.
5. Jones EL, Prosnitz LR, Dewhirst MW, Marcom PK, Hardenbergh PH, Marks LB, Brizel DM, Vujaskovic Z. Thermochemoradiotherapy improves oxygenation in locally advanced breast cancer. Clin Cancer Res 2004;10:4287–4293.
6. Dewhirst MW, Viglianti BL, Lora-Michiels M, Hanson M, Hoopes PJ. Basic principles of thermal dosimetry and thermal thresholds for tissue damage from hyperthermia. Int J Hyperthermia 2003;19:267–294.
7. Dewhirst MW, Vujaskovic Z, Jones E, Thrall D. Re-setting the biologic rationale for thermal therapy. Int J Hyperthermia 2005;21:779–790.
8. Jones E, Thrall D, Dewhirst MW, Vujaskovic Z. Prospective thermal dosimetry: The key to hyperthermia's future. Int J Hyperthermia 2006;22:247–253.
9. Cox RS, Kapp DS. Correlation of thermal parameters with outcome in combined radiation therapy-hyperthermia trials. Int J Hyperthermia 1992;8:719–732.
10. Oleson JR, Samulski TV, Leopold KA, Clegg ST, Dewhirst MW, Dodge RK, George SL. Sensitivity of hyperthermia trial outcomes to temperature and time: Implications for thermal goals of treatment. Int J Radiat Oncol Biol Phys 1993;25:289–297.
11. Sherar M, Liu FF, Pintilie M, Levin W, Hunt J, Hill R, Hand J, Vernon C, Van Rhoon G, Van der Zee J, et al. Relationship between thermal dose and outcome in thermoradiotherapy treatments for superficial recurrences of breast cancer: Data from a phase III trial. Int J Radiat Oncol Biol Phys 1997;39:371–380.
12. Shimm DS, Kittelson JM, Oleson JR, Aristizabal SA, Barlow LC, Cetas TC. Interstitial thermoradiotherapy: Thermal dosimetry and clinical results. Int J Radiat Oncol Biol Phys 1990;18:383–387.

13. Sneed PK, Gutin PH, Stauffer PR, Phillips TL, Prados MD, Weaver KA, Suen S, Lamb SA, Ham B, Ahn DK. Thermoradiotherapy of recurrent malignant brain tumors. Int J Radiat Oncol Biol Phys 1992;23:853–861.
14. Wust P, Rau B, Gellerman J, Pegios W, Loffel J, Riess H, Felix R, Schlag PM. Radiochemotherapy and hyperthermia in the treatment of rectal cancer. Recent Results Cancer Res 1998;146:175–191.
15. Overgaard J, Gonzalez GD, Hulshof MC, Arcangeli G, Dahl O, Mella O, Bentzen SM. Hyperthermia as an adjuvant to radiation therapy of recurrent or metastatic malignant melanoma. A multicentre randomized trial by the European Society for Hyperthermic Oncology. Int J Hyperthermia 1996;12:3–20.
16. Myerson RJ, Perez CA, Emami B, Straube W, Kuske RR, Leybovich L, Von GD. Tumor control in long-term survivors following superficial hyperthermia. Int J Radiat Oncol Biol Phys 1990;18:1123–1129.
17. Myerson RJ, Straube WL, Moros EG, Emami BN, Lee HK, Perez CA, Taylor ME. Simultaneous superficial hyperthermia and external radiotherapy: Report of thermal dosimetry and tolerance to treatment. Int J Hyperthermia 1999;15:251–266.
18. Thrall DE, Larue SM, Yu D, Samulski T, Sanders L, Case B, Rosner G, Azuma C, Poulson J, Pruitt AF, et al. Thermal dose is related to duration of local control in canine sarcomas treated with thermoradiotherapy. Clin Cancer Res 2005;11: 5206–5214.
19. Dewhirst MW, Sim DA, Sapareto S, Connor WG. Importance of minimum tumor temperature in determining early and long-term responses of spontaneous canine and feline tumors to heat and radiation. Cancer Res 1984;44: 43–50.
20. Hand JW, Machin D, Vernon CC, Whaley JB. Analysis of thermal parameters obtained during phase III trials of hyperthermia as an adjunct to radiotherapy in the treatment of breast carcinoma. Int J Hyperthermia 1997;13:343–364.
21. Prionas SD, Kapp DS, Goffinet DR, Ben-Yosef R, Fessenden P, Bagshaw MA. Thermometry of interstitial hyperthermia given as an adjuvant to brachytherapy for the treatment of carcinoma of the prostate. Int J Radiat Oncol Biol Phys 1994;28:151–162.
22. Ryan TP, Trembly BS, Roberts DW, Strohbehn JW, Coughlin CT, Hoopes PJ. Brain hyperthermia: I. Interstitial microwave antenna array techniques – The Dartmouth experience. Int J Radiat Oncol Biol Phys 1994;29:1065–1078.
23. Seegenschmiedt MH, Martus P, Fietkau R, Iro H, Brady LW, Sauer R. Multivariate analysis of prognostic parameters using interstitial thermoradiotherapy (IHT-IRT): Tumor and treatment variables predict outcome. Int J Radiat Oncol Biol Phys 1994;29:1049–1063.
24. Wust P, Stahl H, Loffel J, Seebass M, Riess H, Felix R. Clinical, physiological and anatomical determinants for radiofrequency hyperthermia. Int J Hyperthermia 1995;11:51–167.
25. Albregts M, Hulshof MC, Zum Vorde Sive Vording PJ, van Lanschot JJ, Richel DJ, Crezee H, Fockens P, van Dijk JD, Gonzalez-Gonzalez D. A feasibility study in oesophageal carcinoma using deep loco-regional hyperthermia combined with concurrent chemotherapy followed by surgery. Int J Hyperthermia 2004;20:647–659.
26. van Dijk JD, Schneider C, van Os R, Blank LE, Gonzalez DG. Results of deep body hyperthermia with large waveguide radiators. Adv Exp Med Biol 1990;267:315–319.
27. Westerterp M, Omloo JM, Sloof GW, Hulshof MC, Hoekstra OS, Crezee H, Boellaard R, Vervenne WL, Ten Kate FJ, van Lanschot JJ. Monitoring of response to preoperative chemoradiation in combination with hyperthermia in oesophageal cancer by FDG-PET. Int J Hyperthermia 2006;22:149–160.
28. Van de Kamer JB, de Leeuw AA, Hornsleth SN, Kroeze H, Kotte AN, Lagendijk JJ. Development of a regional hyperthermia treatment planning system. Int J Hyperthermia 2001;17: 207–220.
29. Kok HP, van Haaren PM, Van de Kamer JB, Wiersma J, van Dijk JD, Crezee J. Highresolution temperature-based optimization for hyperthermia treatment planning. Phys Med Biol 2005;50:3127–3141.
30. van Dijk JD, Schneider C, van Os R, Blank LE, Gonzalez DG. Results of deep body hyperthermia with large waveguide radiators. Adv Exp Med Biol 1990;267:315–319.
31. van Haaren PM, Kok HP, Zum Vorde Sive Vording PJ, van Dijk JD, Hulshof MC, Fockens P, van Lanschot JJ, Crezee J. Reliability of temperature and SAR measurements at oesophageal tumour locations. Int J Hyperthermia 2006;22:545–561.
32. van Haaren PM, Kok HP, Van den Berg CA, Zum Vorde Sive Vording PJ, Oldenborg S, Stalpers LJ, Schilthuis MS, de Leeuw AA, Crezee J. On verification of hyperthermia treatment planning for cervical carcinoma patients. Int J Hyperthermia 2007;23:303–314.
33. de Leeuw AA, Crezee J, Lagendijk JJ. Temperature and SAR measurements in deepbody hyperthermia with thermocouple thermometry. Int J Hyperthermia 1993;9:685–697.
34. Kok HP, van Haaren PM, Van de Kamer JB, Zum Vorde Sive Vording PJ, Wiersma J, Hulshof MC, Geijsen ED, van Lanschot JJ, Crezee J. Prospective treatment planning to improve locoregional hyperthermia for oesophageal cancer. Int J Hyperthermia 2006;22:375–389.
35. Hornsleth SN, Mella O, Dahl O. A new CT segmentation algorithm for finite difference based treatment planning systems. In: Franconi C, Arcangeli G, Cavaliere R, editors. Hyperthermic Oncology. Vol. 2. Rome: Tor Vergata; 1996. pp 521–523.
36. ESHO Taskgroup Committee. Treatment planning and modelling in hyperthermia, a task group report of the European society for hyperthermic oncology. Rome: Tor Vergata; 1992.
37. Gabriel C, Gabriel S, Corthout E. The dielectric properties of biological tissues: I. Literature survey. Phys Med Biol 1996;41:2231–2249.
38. Pennes HH. Analysis of tissue and arterial blood temperatures in the resting human forearm. 1948. J Appl Physiol 1998; 85:5–34.
39. van Haaren PM, Kok HP, Oldenborg S, Zum Vorde Sive Vording PJ, Bel A, Geijsen ED, Hulshof MC, Fockens P, van Lanschot JJ, Crezee J. Clinical application of intraluminal hot water balloons combined with locoregional hyperthermia for treatment of oesophageal tumours. Book of Abstracts – 24th annual Meeting of the European Society for Hyperthermic Oncology; 2007;Prague:46–47.
40. Sreenivasa G, Gellermann J, Rau B, Nadobny J, Schlag P, Deuflhard P, Felix R, Wust P. Clinical use of the hyperthermia treatment planning system HyperPlan to predict effectiveness and toxicity. Int J Radiat Oncol Biol Phys 2003;55:407–419.
41. Lyng H, Monge OR, Sager EM, Rofstad EK. Prediction of treatment temperatures in clinical hyperthermia of locally advanced breast carcinoma: The use of contrast enhanced computed tomography. Int J Radiat Oncol Biol Phys 1993; 26:451–457.
42. Overgaard J, Gonzalez GD, Hulshof MC, Arcangeli G, Dahl O, Mella O, Bentzen SM. Randomised trial of hyperthermia as adjuvant to radiotherapy for recurrent or metastatic malignant melanoma. European society for hyperthermic oncology. Lancet 1995;345:540–543.
43. van der Zee J, Gonzalez GD, van Rhoon GC, van Dijk JD, van Putten WL, Hart AA. Comparison of radiotherapy alone with

radiotherapy plus hyperthermia in locally advanced pelvic tumours: A prospective, randomised, multicentre trial. Dutch deep hyperthermia group. Lancet 2000;355:1119–1125.
44. Roemer RB. The local tissue cooling coefficient: A unified approach to thermal washout and steady-state 'perfusion' calculations. Int J Hyperthermia 1990;6:421–430.
45. Kress R, Roemer R. A comparative analysis of thermal blood perfusion measurement techniques. J Biomech Eng 1987;109: 218–225.
46. Sandhu TS. Measurement of blood flow using temperature decay: Effect of thermal conduction. Int J Radiat Oncol Biol Phys 1986;12:373–378.
47. Waterman FM, Tupchong L, Matthews J, Nerlinger R. Mechanisms of heat removal during local hyperthermia. Int J Radiat Oncol Biol Phys 1989;17:1049–1055.
48. Waterman FM, Tupchong L, Liu CR. Modified thermal clearance technique for determination of blood flow during local hyperthermia. Int J Hyperthermia 1991;7: 719–733.
49. Waterman FM, Nerlinger RE, Moylan III DJ, Leeper DB. Response of human tumor blood flow to local hyperthermia. Int J Radiat Oncol Biol Phys 1987;13:75–82.
50. Raaymakers BW, van Vulpen M, Lagendijk JJ, de Leeuw AA, Crezee J, Battermann JJ. Determination and validation of the actual 3D temperature distribution during interstitial hyperthermia of prostate carcinoma. Phys Med Biol 2001; 46:3115–3131.
51. van Vulpen M, Raaymakers BW, de Leeuw AA, Van de Kamer JB, van Moorselaar RJ, Hobbelink MG, Battermann JJ, Lagendijk JJ. Prostate perfusion in patients with locally advanced prostate carcinoma treated with different hyperthermia techniques. J Urol 2002;168:1597–1602.
52. Van den Berg CA, Van de Kamer JB, de Leeuw AA, Jeukens CR, Raaymakers BW, Van VM, Lagendijk JJ. Towards patient specific thermal modelling of the prostate. Phys Med Biol 2006;51:809–825.
53. Song CW. Effect of local hyperthermia on blood flow and microenvironment: A review. Cancer Res 1984;44: 4721s–4730s.
54. Deurenberg P, Weststrate JA, Seidell JC. Body mass index as a measure of body fatness: Age- and sex-specific prediction formulas. Br J Nutr 1991;65:105–114.
55. Taylor RW, Jones IE, Williams SM, Goulding A. Body fat percentages measured by dual-energy X-ray absorptiometry corresponding to recently recommended body mass index cutoffs for overweight and obesity in children and adolescents aged 3–18 y. Am J Clin Nutr 2002;76:1416–1421.